

## Features of structural-phase states of Co-Cr-Al-Y composite coatings after heat treatment

As. Zhilkashinova<sup>1,\*</sup> , M. Skakov<sup>2</sup> , Al. Zhilkashinova<sup>1</sup> ,  
N. Prokhorenkova<sup>3</sup> , M. Abilev<sup>1</sup> 

<sup>1</sup>Sarsen Amanzholov East Kazakhstan University, Ust-Kamenogorsk, Kazakhstan

<sup>2</sup>National Nuclear Center, Kurchatov, Kazakhstan

<sup>3</sup>D. Serikbayev East Kazakhstan Technical University, Ust-Kamenogorsk, Kazakhstan

\*e-mail: a\_zhilkashinova@kemont.kz

(Received 18 March 2022; received in revised form 6 May; accepted 14 June 2022)

This article describes the results of studying the structural-phase state of composite Co-Cr-Al-Y coatings in the initial state and after thermal treatment, obtained because of using the developed magnetron method for applying multilayer coatings with a controlled concentration of constituent elements. According to the results of SEM measurements, it was revealed that unannealed coatings form dense coatings with a columnar structure. The results of transmission electron microscopy confirm the SEM and EDS measurements, and there are clear layer boundaries in the structure for each type of multilayer coating. A distinctive feature of the synthesized layers is the almost complete absence of a crystalline structure for all types of Co-Cr-Al-Y multilayer coatings, which is apparently due to the amorphous properties of cobalt and its tendency to form metallic glasses. The main process occurring during the heat treatment of the studied multilayer coatings is the formation of a spinel-type phase.

The obtained results of experimental studies give new, deeper ideas about the processes of formation of structural-phase states of composite coatings obtained by magnetron sputtering.

**Key words:** coating; structural-phase state; magnetron; phase; spinel; layer-by-layer deposition.

**PACS number:** 82.90.+j

### 1 Introduction

One of the urgent problems in the field of mechanical engineering is the development of technology for improving the strength and performance properties of coating materials for critical parts of power plants [1]. Of great importance is the development of new methods of influencing the structure and properties of coatings, and the complex use of existing developments, the optimal combination of which can create new opportunities for directed influence on the structure and properties of the resulting coatings [2, 3]. At the same time, the structural-phase state has a significant impact on the physical, mechanical and operational properties of coatings.

The vast majority of heat-shielding coatings, including those for gas turbine blades, have an operating principle based on the ability of the surface layer of such coatings to oxidize with the formation of

a protective film based on aluminum oxide  $Al_2O_3$  [4]. The chemical composition (and mainly the amount of aluminum) is the main factor that determines the performance and other protective properties of such coatings [5, 6]. Therefore, in the bulk of the work on the study of heat-shielding coatings, considerable attention is paid to establishing the relationship between the composition of the coating and its protective properties. The relationship between the structure and properties of the coating is analyzed slightly [7].

However, all the accumulated experience in the development and operation of gas turbines shows that, in addition to the chemical composition, one of the most important characteristics of a heat-resistant coating should be considered its structure [8-11]. The coating structure determines not only its strength, ductility, fracture toughness, fatigue resistance, and other properties, but also its heat resistance [12]. Obtaining an optimal structure is

an important condition for achieving the required properties of coatings [13]. Therefore, the further industrial development and widespread use of new effective heat-resistant coatings and progressive fundamentally new technologies for their creation are undoubtedly associated with the need for deep systematic structural studies of these coatings at all stages of their creation and operation, identification of the general patterns of structure formation of both coating materials and the coating itself, the diffusion interaction of the coating with the protected heat-resistant alloy and with the protective oxide film, the processes of change and degradation of the structure under the influence of a wide variety of external factors. These factors determine the role and mechanisms of influence of a particular alloying element or a complex of such elements on the formation of the structure and properties of the coating during deposition and technological heat treatment, on the dynamics of degradation of both structure and properties during operation [14-17].

Methods for studying the states and properties of coatings are widely covered in the literature [18]. Along with a large number of publications devoted to the original research, there are reviews on this topic, monographs, textbooks and reference books [19,20].

However, the above studies were mainly based on coating methods, while studies in terms of the structural-phase state and the relationship between the structure and properties of the coating were not fully investigated.

Along with this, the study of composite coatings is of great interest from a scientific point of view. They can have effects that other materials do not have. The microstructure of a film differs significantly from the structure of a bulk material of the same composition, and the properties of thin films are largely determined by their morphology. Structural defects in bulk materials, which do not significantly affect the properties, in thin films can radically affect their behavior. Surface roughness practically does not affect the characteristics of bulk materials, while for film materials it can be a factor that determines many parameters. Therefore, when studying thin-film materials, it is possible to discover new phenomena and patterns that can become the basis for creating fundamentally new technologies and devices.

At the same time, the analysis showed the relevance of studying the structural-phase state and properties of composite coatings, since at present, in conditions of limited material resources in the

industrial complex, technologies that increase the durability (resource) of machine parts and assemblies are of particular importance.

The aim of this work is to study the structural-phase state of the composite Co-Cr-Al-Y coating obtained by using the developed magnetron method for applying multilayer coatings with a controlled concentration of constituent elements, in the initial state and after heat treatment.

## 2 Materials and methods

The object of the study was Co-Cr-Al-Y multilayer coatings (1-, 2-, 4-, and 8-layers), which were deposited on a single-crystal silicon substrate with [100] crystallographic orientation.

The coatings were deposited by the magnetron method on an ion-plasma setup, which was a vacuum chamber with two magnetron-sputtering systems of an unbalanced type and an ion source with a closed electron drift [21].

The structural-phase state and elemental composition were determined by scanning electron microscopy using a JEOL-2200FS (Japan) (EDX) INCA ENERGY scanning electron microscope (Oxford Instruments, UK). Accelerating voltage was up to 30 kV; resolution was up to 3 nm, instrumental magnification was up to x300,000. Samples were placed in a mold with a diameter of 30 mm, filled with epoxy filler, dried, and then the resulting puck was ground and polished.

The structure and microstructure of the annealed samples were studied using a ThemisZ electron microscope (Thermo Fisher Scientific, USA) with an accelerating voltage of 200 kV and a limiting resolution of 0.07 nm. Images were recorded using a Ceta 16 CCD array (Thermo Fisher Scientific, USA). The instrument is equipped with a SuperX (Thermo Fisher Scientific, USA) energy-dispersive characteristic X-ray spectrometer (EDX) with a semiconductor Si detector with an energy resolution of 128 eV.

Sample preparation for TEM studies was reduced to obtaining a cross section by grinding with etching. A scratch was applied with a scribe (Fine Point Diamond Scribe 54467, Ted Pella, USA) to the substrate on the reverse side of the sample. The coated substrate is cleaved along the scratch line by applying the required scalpel pressure. Bonding of individual parts takes place with the front sides (films on substrates) in such a way that two ends

become visible. A special epoxy two-part adhesive EpoxyBond 110TM 2-Part Adhesive manufactured by Allied High Tech Products, Inc. was used.

A quartz cylinder with a diameter of 5 mm was used. Wax was applied on the surface of this cylinder and a gluing of the samples was attached with the ends up. Then the sample was polished at the LEICA EM TXP grinding and polishing plant. The samples were subjected to additional thinning using ion etching. The copper ring with the sample was placed in a special holder for the Gatan Precision ION polishing system model 691 ion etching station. The sample was placed in the microscope holder EM-21010/21020: Single Tilt Holder for TEM JEOL-2200FS (JEOL, Japan) (Figure 1).

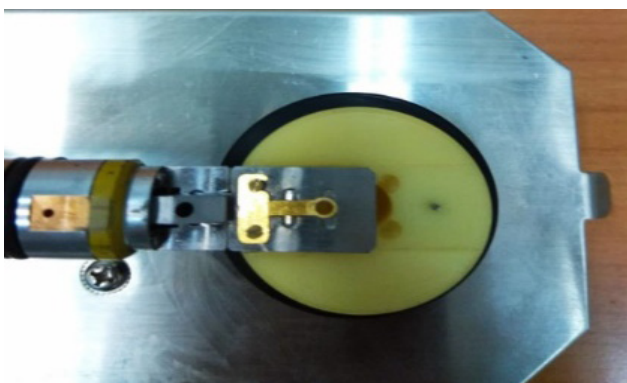


**Figure 1** – Sample holder EM-21010/21020: Single Tilt Holder for TEM JEOL-2200FS.

X-ray phase analysis was performed on a Shimadzu XRD 6000 instrument with a Cu anode  $K\alpha$  ( $\lambda = 0.154$  nm) by the grazing beam method (shooting angle  $15^\circ$ ) in the range  $2\theta = 20-80^\circ$ . Due to the low intensity of the peaks, the initial signal was approximated by Gaussian curves. Studies were also carried out using the X-ray powder diffraction method on the ARLX'tra instrument (ThermoFisher Scientific). The sample before each shooting was fixed with glue on an amorphous polycarbonate cuvette. Shooting of film samples was performed using symmetrical (Bragg-Brentano) geometry, in the angle range of  $15-70^\circ$ , and asymmetric geometry, in the range of  $20-50^\circ$ . The PDF-2 database compiled by the International Committee on Diffraction Data JCPDS (ICDD) was used as a reference file.

The heat treatment of the coatings was carried out on a MILA-5000 unit (ULVAC-RICO (Japan),

equipped with IR halogen lamps with a total power of 4 kW and a maximum radiation intensity in the range of  $0.8-1.2$   $\mu\text{m}$ . The unit allows operation in the temperature range from up to  $1000$   $^\circ\text{C}$  with a maximum temperature increase rate of  $100$   $^\circ\text{C}/\text{min}$ . On this installation, work was carried out to heat the samples at  $400$   $^\circ\text{C}$ ,  $800$   $^\circ\text{C}$  and  $1000$   $^\circ\text{C}$ . The heating took place in a programmed mode with a given rate of reaching the desired temperature, as well as during the transition from one annealing temperature to another. The annealing time at a given temperature or sequentially at several temperatures also passed in the programmed mode.

### 3 Results and discussion

The study of the structure and composition of multilayer coatings was carried out using electron microscopy. One of the results of the study of the cross section of coatings and the corresponding energy dispersive spectrum is shown in Figure 2.

According to the results of SEM measurements, it was revealed that the Co-Cr-Al-Y system forms dense coating with a columnar structure typical for metal coatings. The images on Figure 2 show that during the deposition process a coating was formed, which has a high-relief character. The thickness of all synthesized Co-Cr-Al-Y coatings varies within  $2.0 \pm 0.2$   $\mu\text{m}$ , and the thickness of an individual layer is  $0.4$   $\mu\text{m}$ . The distribution of the constituent elements of the coating from point to point practically does not change. We believe that the presence of silicon atoms in the composition of the coatings is due to it's getting there precisely from the detection of the substrate itself, since the distribution of silicon atoms over the depth and width of the coating is uniform. The presence of an oxygen peak in the EDS spectrum is due to its adsorption on the cut surface after removal from the vacuum chamber.

Transmission microscopy results confirm the SEM and EDS measurements. Figures 3 and 4 show transmission microscopy images and corresponding elemental mapping. Elemental mapping by constituent elements showed that with a relatively uniform distribution of Al and Y in the thickness of the coating, the layers of enriched/depleted Co/Cr alternate in accordance with the parameters of magnetron sputtering described in [22, 23]. A large amount of Y in the substrate during elemental mapping is associated with the superposition of the spectra of Y and Si in the EDS spectrum.

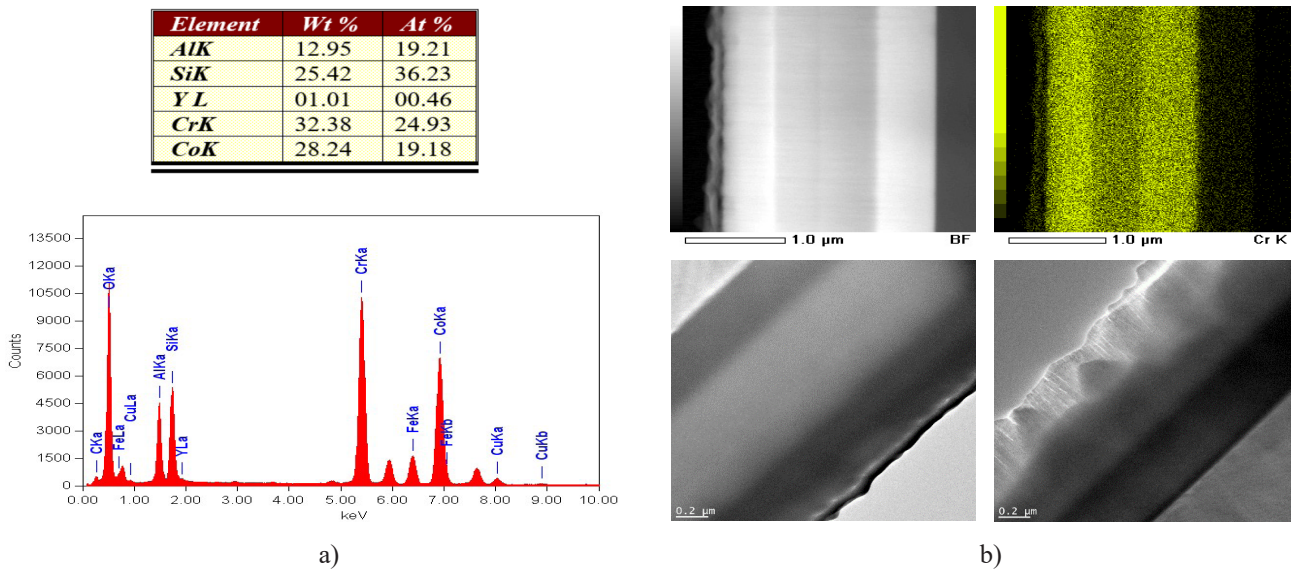


**Figure 2 – An energy dispersive spectrum (a) of the coatings and SEM images of a cross section of the coating (four-layer coating) (b).**

A distinctive feature of the synthesized layers is the almost complete absence of a crystalline structure for all types of synthesized multilayer Co-Cr-Al-Y coatings, which is most likely due to the amorphous properties of cobalt and its tendency to form metallic glasses.

Figure 4 shows that the structure of the samples is columnar, microcracks are noticeable, which may indicate the presence of microstresses in the film, while ion etching showed these microstresses. However, it is possible that ion etching slightly destroys the film during thinning, and microcracks may be a consequence of the destruction of the film surface.

Film layering is also clearly visible in all TEM images. In the STEM mode, the number of layers is displayed more clearly, the boundaries of all layers are clear, which means that the process of layer growth during deposition took place in the optimal mode.

Elemental analysis showed that Co and Cr are distributed in the layers in the form of a gradient. At the same time, the content of Co in a single-layer coating is the maximum value – 27.63%, in a 4-layer coating – the minimum value – 19.4%. The chromium content, on the contrary, increases with the increase in the number of layers. So, in a single-layer coating, this value is 18.82%, and in an 8-layer coating – 24.15%. Aluminum is evenly distributed over all layers of the film. Its content remains largely

unchanged. In a 1-layer coating – 9.75%, 4-layer – 8.85%. Yttrium is located in the form of a small thin layer at the film/substrate interface; during thinning with the help of ion argon guns, it is etched away until destruction (EDS detects a weak peak that “merges” with a large silicon peak). The silicon content in the coating in 1, 2 and 4-layer coatings is in the range of 5.00 – 5.44%. In this case, in an 8-layer coating, this value is 3.89%. This is due to the formation of a diffuse region at the film–substrate interface. The oxygen content in the multilayer coating was found to be in the range of 10-20%. The presence of oxygen in the surface layer of the coatings is due to its adsorption on the cut surface after removal from the vacuum chamber, as well as after argon etching.

Figure 5 shows the results of X-ray phase analysis by the method of a grazing beam of coating samples of 4- and 8-layer coatings.

For all synthesized Co-Cr-Al-Y coatings, the main peaks can be distinguished:  $2\theta \approx 30^\circ$  and  $57^\circ$ , corresponding to the peaks of the first and third order of the silicon substrate (111). Dominant peak of Cr (110) at  $2\theta \approx 43^\circ$ , pronounced for multilayer coatings of 2- and 8-layers and much less intense for a single-layer coating. This correlates with the significantly lower Cr concentration in the single layer coating measured from the EDS results. Fourth order peaks are Y(411) and Y(444). The absence of Co and Al peaks is probably because they form an X-ray amorphous layer, which is confirmed by the results



of TEM. Summing up the results of TEM and XRD, we can state the formation of an amorphous Co/Al matrix with Cr and Y nanocrystals distributed in the

thickness of the coating. The formation of intermetallic compounds in the deposited Co-Cr-Al-Y system was not detected.

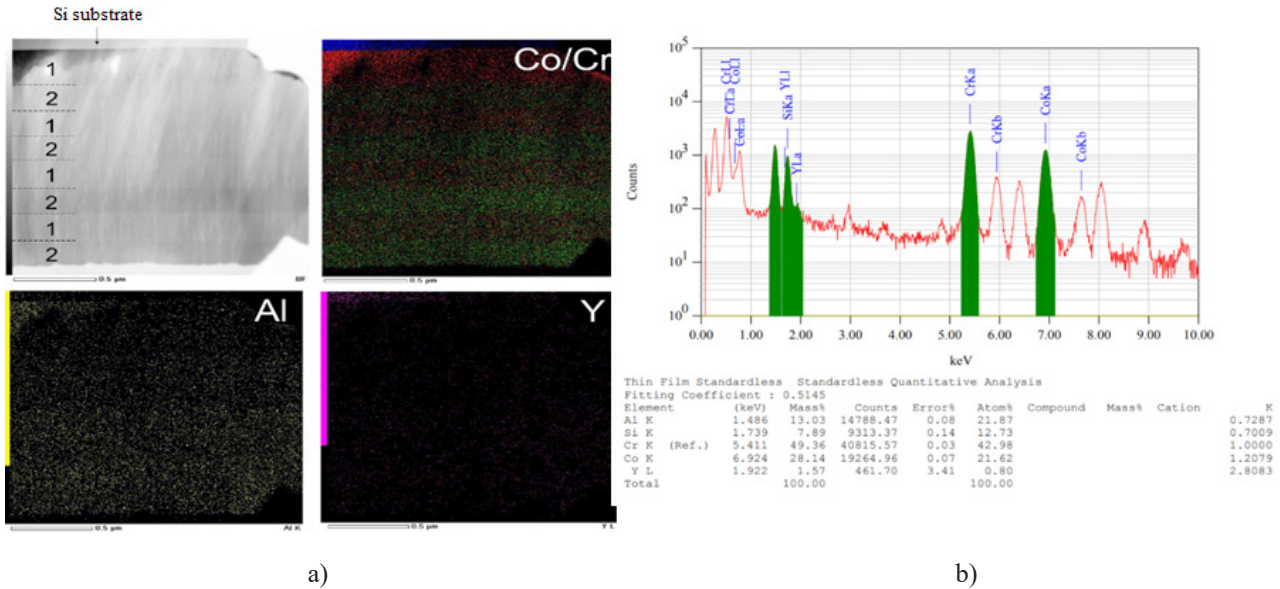


Figure 3 – TEM images of the cross section of the coating (a) and its elemental mapping (four-layer coating) (b)

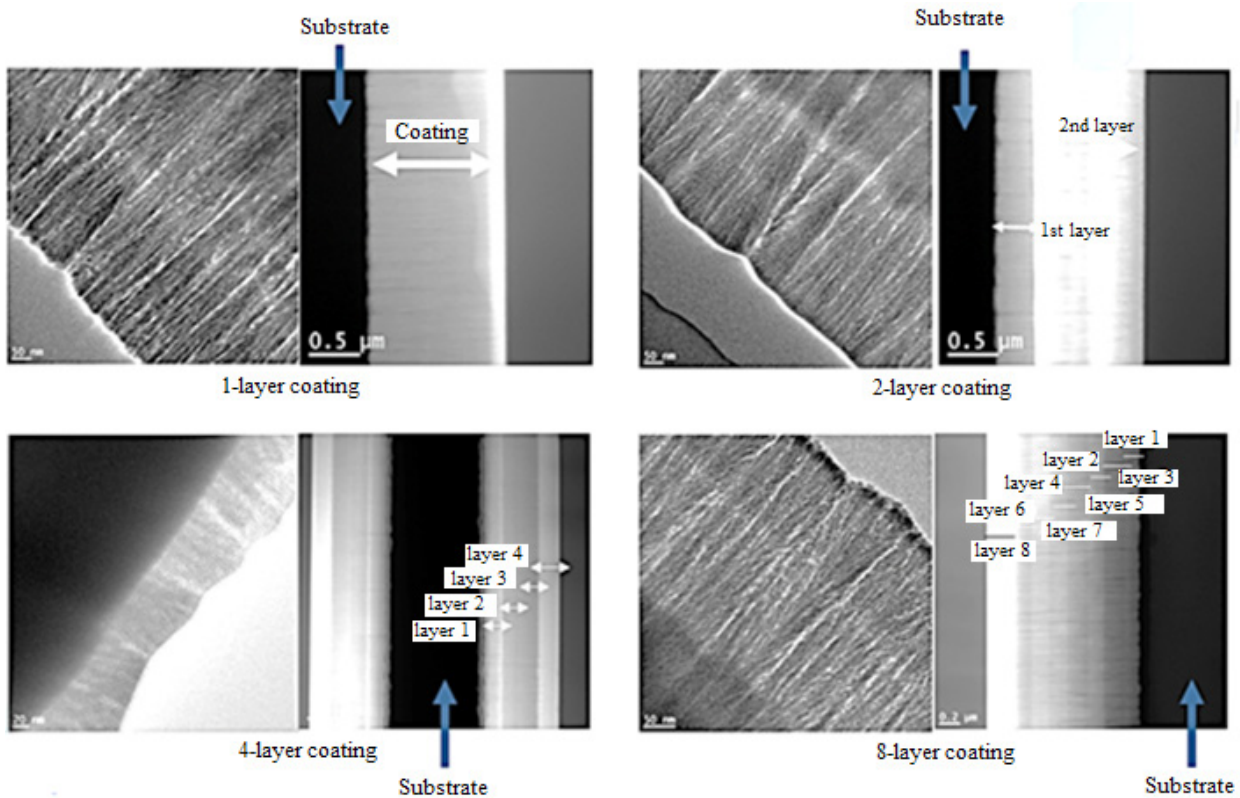


Figure 4 – Microstructure of various sections of all series of coatings

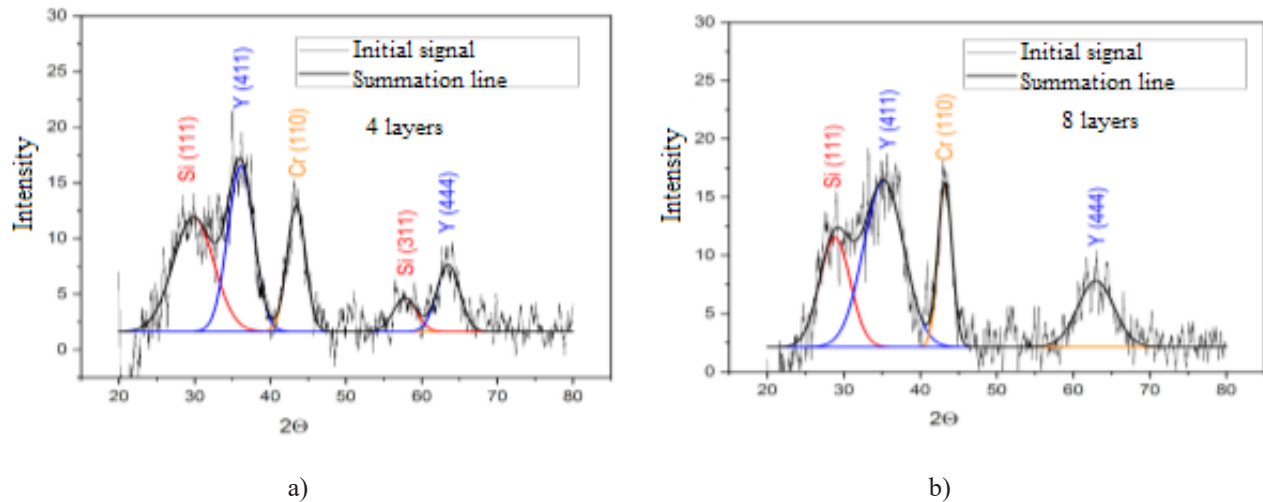


Figure 5 – X-ray phase analysis: (a) four-layer coating; (b) eight-layer coating

The results of studies of the structural-phase state of Cr-Al-Co-Y coatings because of thermal treatment in an Ar medium at 400 °C showed some changes in comparison with untreated samples. In the case of the single-layer sample, it was not possible to detect extraneous reflections except for the reflections of the silicon substrate 111 and 220. These reflections are mainly due to the defocus of the incident beam on the sample at small angles of incidence. However, for the remaining samples, the appearance of reflections of a number of phases was noticed:  $\text{SiO}_2$ ,  $\text{CoO}$ ,  $\text{AlSi}_{0.5}\text{O}_{2.5}$ , and  $\text{CrAl}_{0.42}\text{Si}_{1.58}$ .

A further increase in the annealing temperature in Ar at 800°C does not lead to significant changes. In the case of a sample consisting of two composite layers, the reflections of various impurity phases disappeared and the  $\text{Co}_3\text{O}_4$  phase was formed. It should be noted that the  $\text{CoCr}_2\text{O}_4$  phase, which also has a spinel-type structure, has a similar set of reflections in position and intensity, and the elemental analysis data showed a fairly homogeneous distribution of chemical elements in the material. In this regard, overlapping of peaks in the diffractogram may occur, and this phase, meanwhile, may be present in the sample. In the case of the sample with eight layers of the

composite, the formation of a phase similar to  $\text{Y}_2\text{O}_3$  was also observed.

For samples annealed at 1000 °C, the formation of a spinel-type phase ( $\text{Co}_3\text{O}_4\text{-CoCr}_2\text{O}_4$ ) was observed in all cases. In the sample with two layers, impurities were also found similar to those observed at lower annealing temperatures, but were not observed for the sample annealed at 800°C. In this case, this is because the samples had different areas and, therefore, contained different amounts of the substance, based on which the reflections of impurity phases could not be observed in the case of one sample, but the phases themselves could be preserved. In the case of 2-layer and 4-layer composites, the yttrium oxide phase was detected (Figure 6).

The structure of the samples, as well as in the unannealed ones, is columnar, the same microcracks are observed as in the unannealed samples. The layers are clearly distinguishable on the TEM, STEM images, and on the EDS maps. There is a “mixing” of elements in the layers of annealed samples (Figure 7).

Similarly, to the previous series (annealed at 400°C), there is a “mixing” of elements in the film layers.

The structure of the samples annealed at 1000°C is shown in Figure 8.

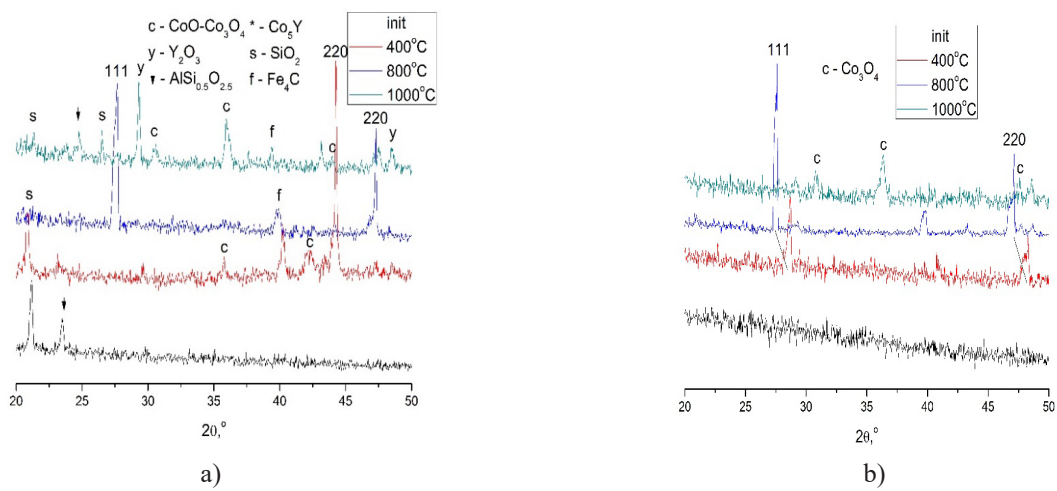


**Figure 6** – X-ray diffraction patterns of the Y-Co-Al-Cr sample in asymmetric geometry depending on the annealing temperature of the samples: (a) – single-layer; (b) – four-layer coatings

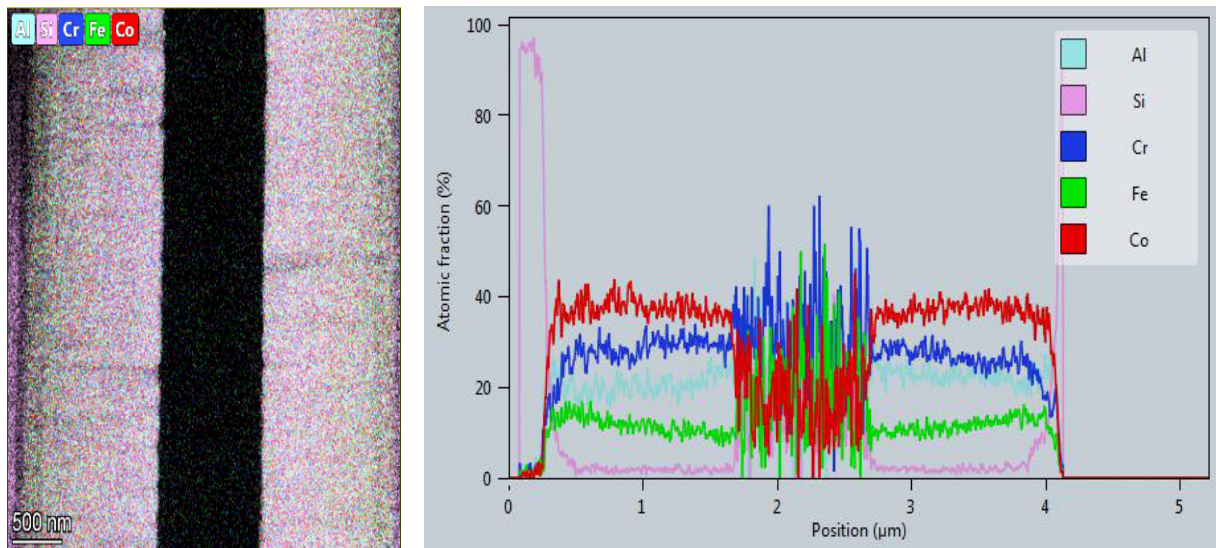


**Figure 7** – EDS analysis of single-layer coating at 1000 °C

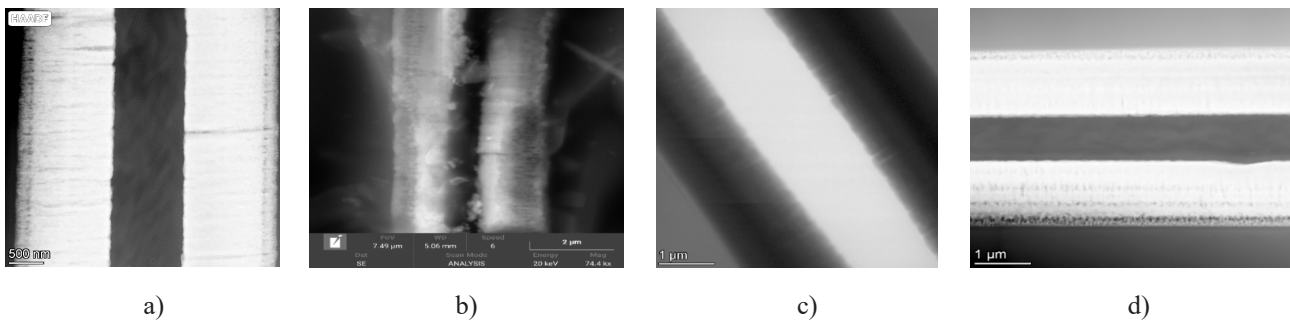


**Figure 8** – Structure of samples annealed at 1000°C: (a) 1-layer; (b) 2-layer; (c) 4-layer; (d) 8-layer samples.



The structure is similar to all previous samples; the presence of layers is clearly distinguishable in all modes of TEM (also SEM). As with the previous annealed samples, mixing of the film layers is noticeable. The silicon content in the coatings after heat treatment increased significantly – more than 10 times. This applies to 1-layer coating (400°C) – 29.52%, 2-layer coating (400°C) – 33.10%. It was observed that the cobalt content decreases with increasing annealing temperature. So, for 1, 2, 4 and 8-layer coatings annealed at a temperature of 400°C, the cobalt content is 31.30; 17.10; 7.57; 3.58% respectively. For 1, 2, 4, and 8-layer coatings annealed at 800°C, the cobalt content is 4.00; 19.91; 4.50; 10.37% respectively. Aluminum is distributed evenly over all layers of the film. The maximum content of Al in 1-layer coatings subjected to thermal treatment at temperatures of 400 and 1000°C. The minimum value for the Al content is set in the 8-layer coating (400°C) – 1.49%. In the remaining samples, this figure ranges from 3.60 to 8.22%. Chromium and cobalt are distributed in a gradient. The average value of the chromium content is generally similar to samples without thermal treatment. However, it has been found that for 8-layer (400°C), 1-layer (800°C) and 2-layer (1000°C), the chromium content is 1.38, 3.20 and 4.60%, respectively. After heat treatment of coatings, it was possible to establish the content of Y: in 1-layer (400°C) – 0.72%, in 8-layer (400°C) – 0.04%, in 1-layer (1000°C) – 0.97%, in 4-layer (1000°C) – 0.32%, in 8-layer (1000°C) – 0.52%. At an annealing temperature of 400°C, the oxygen content in 1 and 8 layer coatings was not established, similarly for 1 and 4 layer coatings at a processing temperature of 1000°C. The oxygen content in 2 and 4 layer coatings at the annealing temperature is 25.80 and 45.82%, respectively. As noted above, the presence of oxygen in the surface layer of the coatings is due to its adsorption on the cut surface after being removed from the vacuum chamber.

#### 4 Conclusions

The structural-phase state before and after heat treatment of multilayer Co-Cr-Al-Y coatings on a silicon substrate, obtained by the magnetron method, has been studied. According to the results of SEM measurements, it was revealed that unannealed coatings form dense coatings with a columnar structure typical for metal coatings. The total thickness of one layer of the composite coating, which includes se-

quential Co-Cr-Al-Y components, ranges from  $2.0 \pm 0.2 \mu\text{m}$ , and the thickness of a separate sublayer of each element is  $0.4 \mu\text{m}$ . The study of the local and integral elemental composition of coatings shows that the matrix has a gradient character. According to the data of energy dispersive analysis, the concentration of chromium in the coating increases with an increase in the number of layers, with a proportional decrease for cobalt, which is associated with the influence of the second layer with an increased concentration of chromium.

Transmission microscopy results confirm the SEM and EDS measurements. The structure contains clear layer boundaries for each type of multilayer coating. Elemental mapping by constituent elements showed a relatively uniform distribution of Al and Y in the thickness of the coating and layers of enriched/depleted Co/Cr alternate. A large amount of Y in the substrate during elemental mapping is associated with the superposition of the spectra of Y and Si in the EDS spectrum. A distinctive feature of the synthesized layers is the almost complete absence of a crystalline structure for all types of synthesized Co-Cr-Al-Y multilayer coatings, which is associated with the amorphous properties of cobalt and its tendency to form metallic glasses.

For all Co-Cr-Al-Y coatings, the main peaks can be distinguished:  $2\theta \approx 30^\circ$  and  $57^\circ$ , corresponding to the peaks of the first and third order of the silicon substrate (111). Dominant peak Cr (110) at  $2\theta \approx 43^\circ$ , pronounced for multilayer coatings of 2-8 layers and much less intense for a single-layer coating. This correlates with the significantly lower Cr concentration in the single layer coating measured from the EDS results.

The results of studies of the structural-phase state of Cr-Al-Co-Y coatings after the heat treatment in an Ar medium at  $400^\circ\text{C}$  showed some changes in comparison with untreated samples. The appearance of reflections of a number of phases was noticed:  $\text{SiO}_2$ ,  $\text{CoO}$ ,  $\text{AlSi}_{0.5}\text{O}_{2.5}$ , and  $\text{CrAl}_{0.42}\text{Si}_{1.58}$ . A further increase in the annealing temperature in Ar at  $800^\circ\text{C}$  does not lead to significant changes. For samples annealed at  $1000^\circ\text{C}$ , the formation of a spinel-type phase ( $\text{Co}_3\text{O}_4\text{-CoCr}_2\text{O}_4$ ) was observed in all cases. In the sample with two layers, impurities were also found similar to those observed at lower annealing temperatures, but were not observed for the sample annealed at  $800^\circ\text{C}$ .

Based on the data obtained, it can be stated that the main process occurring during the annealing of



these composites is the formation of a spinel-type phase. In this case, despite the symbol  $\text{Co}_3\text{O}_4$ , the composition of the resulting spinel may be different, and may include Cr, Y, and Al, based on the possible charge states of these cations ( $\text{Cr}^{3+}$ ,  $\text{Al}^{3+}$ ,  $\text{Y}^{3+}$ ). Their final formation for all samples occurs in the temperature range of 800-1000°C. In this case, the yttrium oxide phase can form separately from particles with this structure, which is due to the large size of the  $\text{Y}^{3+}$  cation. Apparently, one of the main reasons for the formation of spinel structures is the partial acidification of films, which was already demonstrated for the initial amorphous samples by the TEM method, and the uniform character of oxygen saturation of the layers indicates that the samples were acidified at the

stage of their deposition onto the substrate. The calcination of samples in an inert atmosphere does not lead to the reduction of oxides, but to their crystallization. This allowed to conclude that in the future, to obtain composite layers by heat treatment, it is necessary to use a medium with a more reducing character, for example, a mixture of  $\text{Ar} + \text{H}_2$  or  $\text{He} + \text{H}_2$  gases, which will contribute to the reduction of the original spinels.

### Acknowledgment

This research is funded by the Science Committee of the Ministry of Education and Science of the Republic of Kazakhstan (Grant No. AP08053322).

### References

1. B. Bhushan. Principles and applications of tribology // *Industrial Lubrication and Tribology* -1999. -Vol. 51. -No. 6. -P. 313-313. <https://doi.org/10.1108/ilt.1999.51.6.313.1>
2. S.Ya. Betsofen, L.M. Petrov, Su S. K., A.N. Lutsenko. Study of the structure of protective coatings on a nickel heat-resistant alloy // 6th Int. Conf. "Films and Coatings'2001": Proceedings. report -SPb., 2001. – P. 477-482.
3. N.A. Khaponen, A.S. Lisyansky. Survivability of turbines near and beyond the park resource // *Safety of labor in industry*. – 2004. – No. 7. – P.16 (in Russian).
4. V.I. Gladshtein. Influence of operating time up to 350 thousand hours on service characteristics and structure of cast housing parts of steam turbines and fittings // *Metal Science and Thermal Processing of Metals*. – 2007. – No. 2. – P.21-23 (in Russian).
5. A.A. Smirnov, S.A. Budinovskiy, P.V. Matveev, D.A. Chubarov. Development of heat-shielding coatings for HPT blades from nickel single-crystal alloys VZHM4, VZHM5U // *Proceedings of All-Russian Research Institute of Aviation Materials*, No. 1, 2016, P.17-24 (in Russian).
6. V. Kumar, A. M. Vijay, J. J. Duthie, S. Archan. Analyzing and establishing the protective coating for low pressure turbine blades of Adour MK811 engine, Project Report, Bachelor of Engineering, Department of Aeronautical Engineering, Kumaraguru College of Technology, Coimbatore-49, India, April 2011.
7. P. Zhang, K. Yuan, R. L. Peng, X.-H. Li, S. Johansson. Long-term oxidation of MCrAlY coatings at 1000 C and an Al-activity based coating life criterion // *Surface and Coatings Technology*. – 2017. -Vol. 332. -No.25. -P. 12-21. <https://doi.org/10.1016/j.surfcoat.2017.09.086>
8. H.S. Nithin, Vijay Desai, M.R. Ramesh. Elevated temperature solid particle erosion behaviour of carbide reinforced CoCrAlY composite coatings // *Materials Research Express*. -2018. -Vol. 5. -P. 066529. <https://doi.org/10.1088/2053-1591/aac998>
9. G.A. Bleykher et al. Features of copper coatings growth at high-rate deposition using magnetron sputtering systems with a liquid metal target // *Surface and Coatings Technology*. – 2017. – Vol. 324. – P. 111–120. <https://doi.org/10.1016/j.surfcoat.2017.05.065>
10. A.V. Yuryeva et al. Effect of material of the crucible on operation of magnetron sputtering system with liquid-phase target // *Vacuum*. – 2017. – Vol. 141. – P. 135– 138. <https://doi.org/10.1016/j.vacuum.2017.04.001>
11. B. Rakhadilov, M. Maulet, M. Abilev, Z. Sagdoldina, R. Kozhanova. Structure and tribological properties of Ni–Cr–Al-Based gradient coating prepared by detonation spraying // *Coatings*. – 2021. -Vol. 11. -P. 218. <https://doi.org/10.3390/coatings11020218>
12. H. Ikezi. Coulomb solid of small particles in plasmas // *The Physics of Fluids*. – 1986. – Vol. 29. – N. 6. – P. 1764-1766. <https://doi.org/10.1063/1.865653>
13. L. Wang, X.H. Zhong, Y.X. Zhao, S.Y. Tao, W. Zhang, Y. Wang, X.G. Design and optimization of coating structure for the thermal barrier coatings fabricated by atmospheric plasma spraying via finite element method // *Journal of Asian Ceramic Societies*. -2014. -Vol. 2. -P.102-116. <https://doi.org/10.1016/j.jascer.2014.01.006>
14. S. A. Khrapak, B. A. Klumov, P. Huber, V. I. Molotkov, A. M. Lipaev, V. N. Naumkin, A. V. Ivlev, H. M. Thomas, M. Schwabe, G. E. Morfill, O. F. Petrov, V. E. Fortov, Y. Malentschenko, S. Volkov. Fluid-solid phase

transitions in three-dimensional complex plasmas under microgravity conditions // *Physical Review E*. -2012. -Vol. 85. -N. 6. -P. 66-75. <https://doi.org/10.1103/PhysRevE.85.066407>

15. 15. I. Tacikowski, I. Sutkowski, J. Senatorski, J. Michalski. Modyfikowane warstwy azotowane wytwarzane w procesie regulowanym. porfczonym z utwardzaniem cieplnym podtoza // *Inzynieria Materialowa*. -2000. -Vol. 22. -P. 449-452. (in Polish).

16. 16. A. Karakurkchi, N. Sakhnenko, R. Atchibayev. Research on the improvement of mixed titania and Co(Mn) oxide nano-composite coatings // *IOP Conference Series: Materials Science and Engineering*. -2018. -P. 69-74.

17. 17. M. Ved' , N. Sakhnenko, I. Yermolenko. Composition and corrosion behavior of iron-cobalt-tungsten // *Eurasian Chemico-Technological Journal*. -2018. -Vol.20(3).- P. 145-152.

18. 18. G. Yar-Mukhamedova, N. Sakhnenko. Nano-composition Ti-Co(Mn) coatings investigation // *International Multidisciplinary Scientific GeoConference Surveying Geology and Mining Ecology Management, SGEM*. -2018. -P. 1-15

19. 19. A. Zhilkashinova, M. Abilev, A. Pavlov, N. Prokhorenkova, M. Skakov, A. Gradoboev, A. Zhilkashinova. Ion-plasma spraying and electron-beam treatment of composite Cr-Al-Co-ZrO<sub>2</sub>-Y<sub>2</sub>O<sub>3</sub> coating on the surface of Ni-Cr alloy, coatings. -2021. -Vol.11(3). -P. 321. <https://doi.org/10.3390/coatings11030321>

20. 20. A. Zhilkashinova, M. Skakov, A. Zhilkashinova, A. Gradoboyev. Multilayer ion-plasma coating CR-AL-CO-Y and its phase composition // *Reports of the national academy of sciences of the Republic of Kazakhstan*. -2021. -Vol. 4.-No. 338. -P. 158 - 166. <https://doi.org/10.32014/2021.2518-1483.73>

21. 21. A. Zhilkashinova, M. Skakov, A. Zhilkashinova, I. Ocheredko. Computational – experimental method of forecasting the lifetime of CO-CR-AL-Y composite coatings // *Reports of the national academy of sciences of the Republic of Kazakhstan*. -2022. -Vol. 1. -N. 341. -P. 117–123. <https://doi.org/10.32014/2022.2518-1483.140>

22. 22. S.Klemme, J.C. Miltenburg. The heat capacities and thermodynamic properties of NiAl<sub>2</sub>O<sub>4</sub> and CoAl<sub>2</sub>O<sub>4</sub> measured by adiabatic calorimetry from T = (4 to 400) K // *Journal of Chemical Thermodynamics*. -2009. -Vol. 41. -P. 842–848

23. 23. J. Li, X. Zhou, Y. Liu, Y. Chen, J. Zhang, R. Huang, J. Tan, Z. Li, B. Yang. Effects of different post-treatments on arc erosion resistance of cold-sprayed AgC composite electric contact // *Coatings*. -2021. -Vol. 11. -P. 363. <https://doi.org/10.3390/coatings11030363>

© This is an open access article under the (CC)BY-NC license (<https://creativecommons.org/licenses/bync/4.0/>).  
Funded by Al-Farabi KazNU